Timing Synchronization for Real-Valued Orthogonal Space-Time Block Codes

Pawel A. Dmochowski, Peter J. McLane

Department of Electrical and Computer Engineering

Queen's University, Kingston, ON, K7L 3N6, Canada

Email: pdmochowski@ieee.org, mclanep@post.queensu.ca

Abstract— **Low complexity timing error detectors for rate one orthogonal space-time block codes with real modulation are presented. For 2-, 3- and 4-transmit antenna codes, we derive robust timing error estimators and obtain analytical expressions for the estimation error variance and the signal-to-noise ratio. The performance is evaluated by examining the estimator's tracking capabilities in a system operating over a frequency-flat Rayleigh fading environment. The bit-error-rate results are presented showing degradation due to timing synchronization of less than 0.5 dB. In addition, we study the performance as a function of the timing drift and show that the timing loop is able to track up to normalized timing drift bandwidth of 0.001. Perfect channel state information at the receiver is assumed throughout the paper.**

I. INTRODUCTION

As in conventional single-antenna communications, the estimation of reference parameters, such as timing epoch and the channel state, is critical to the performance of MIMO receivers. Timing acquisition in space-time coded modems was first addressed in [1], where the receiver obtained timing information by maximizing the oversampled log-likelihood function (LLF) derived from an orthogonal training sequence. A modification of the method in [1] was presented in [2] and [3] where the resulting algorithm reduces the required oversampling rate.

In contrast to the works in [1], [2] and [3], which deal with the problem of coarse timing acquisition, this paper focuses on low complexity timing tracking without the knowledge of data at the receiver. A framework for the design of timing error detectors (TED's) suitable for orthogonal space-time block coded (OSTBC) receivers was laid out in [4], where the estimation variance and the output signal-to-noise ratio (SNR) were also derived. The analysis in [4] was an extension of the results in [5] and [6] which were restricted to the case of Alamouti codes for 2 transmit antennas. In this paper we describe TED's for 2-, 3- and 4-transmit antenna OSTBC with real modulation formats.

The remainder of this paper is organized as follows. We begin with a system overview in Section II. The theory of timing error detector design for OSTBC is summarized in Section III, where analytical expressions for the S-curve and estimation error variance are given along with examples of TED's. Simulation results are presented in Section IV with bit-error-rate (BER) performance shown in Section IV-B and

timing bandwidth range in Section IV-C. We conclude with a summary of findings in Section V.

II. SYSTEM OVERVIEW

We consider an orthogonal space-time block coding communication system with N_t transmit and N_r receive antennas. The transmitter encodes N_s information symbols and transmits them over N_t antennas in N_c time slots, resulting in a code rate of $R = N_s/N_c$. We denote the lth $N_t \times N_c$ code block by $\mathbf{X}_l$ and its (i,k)th entry by $x_i(lN_c + k)$. Note that l is the code block index, $k = 0, \ldots, N_c - 1$ is the time slot index within the block and $i = 1, \ldots, N_t$ is the transmit antenna index. Let the mth information symbol used to encode block $\mathbf{X}_l$ be a_m^l, where $m = 0, \ldots, N_s - 1$. For real-valued data, $\mathbf{X}_l$ is given by the linear combination of a_m^l [7]

$$\mathbf{X}_l = \sum_{m=0}^{N_s-1} a_m^l \mathbf{A}_m, \qquad (1)$$

where $\mathbf{A}_m$ represents integer code matrices obtained from orthogonal designs.

Following the encoding, data on each transmitter branch is passed through a pulse shaping filter. The pulse shaping is split between the transmitter and the receiver, each with a root raised cosine (RRC) filter denoted by $\tilde{g}(t)$. The combined Nyquist raised cosine pulse is represented by $g(t) = \tilde{g}(t) * \tilde{g}(t)$, where $*$ denotes convolution. We assume a frequency-flat Rayleigh fading channel modeled by a $N_r \times N_t$ matrix $\mathbf{H}$. It's components, denoted by h_{ij}, correspond to the state of the channel from ith transmit to jth receive antenna and are assumed to be independent and identically distributed (iid) for all i and j. A U-shaped power spectrum is assumed and thus the autocorrelation of h_{ij} (for all i and j) is given by [8]

$$R_h(\xi) = \sigma_h^2 J_0(2\pi f_D \xi), \qquad (2)$$

where σ_h^2 is the variance of the random process and $J_0(x)$ denotes the Bessel function of the first kind of order zero. The quantity f_D in (2) denotes the maximum Doppler frequency which is assumed to be known.

The receiver diagram is shown in Figure 1. The signal at antenna j is given by

$$r_j(t) = \sum_{i=1}^{N_t} h_{ij}(t) \sum_{n'} x_i(n')\tilde{g}(t - n'T) + \tilde{\eta}_j(t), \qquad (3)$$
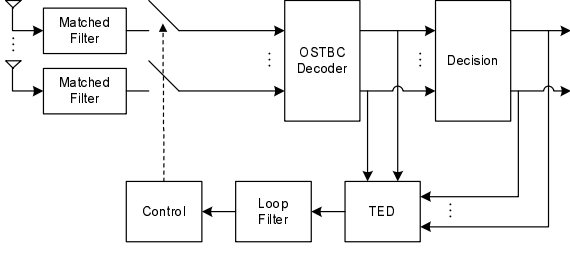
Fig. 1. Receiver Diagram.

where $x_i(n')$ is the encoded symbol transmitted by antenna i at time $n' = lN_c + k$ and $\tilde{\eta}_j(t)$ is a zero mean complex Gaussian noise with variance $\sigma_{\tilde{\eta}}^2 = N_0/2$. The matched filtered signal $y_j(t) = r_j(t) * \tilde{g}(t)$ is sampled at time instants $t_n = nT + \epsilon$, where ϵ is the unknown timing error, assumed to be equal on all branches. We express ϵ by $\epsilon = \tau - \hat{\tau}$, where τ is the timing offset at the receiver and $\hat{\tau}$ is the correction applied by the timing synchronization algorithm. Assuming the channel fading is sufficiently slow, such that $h_{ij}(t_n) \approx h_{ij}(nT) \triangleq h_{ij}(n)$, the resulting samples are given by

$$y_j(n) = \sum_{i=1}^{N_t} h_{ij}(n) \sum_{n'} x_i(n')g(nT - n'T + \epsilon) + \eta_j(n), \quad (4)$$

where $\eta_j(n)$ are the samples of the filtered noise $\eta_j(t) = \tilde{\eta}_j(t) * \tilde{g}(t)$, which are uncorrelated if sampled at the symbol rate.

We assume that the timing error ϵ is constant for the duration of one code block. Similarly, we assume quasi-static fading, where $h_{ij}(lN_c) \approx h_{ij}((l+1)N_c - 1)$. One can show [4] that for a single block l, the output samples can be expressed by an $N_r \times N_c$ matrix $\mathbf{Y}_l$,

$$\mathbf{Y}_l = \mathbf{H}_l \mathbf{X}_{\epsilon,l} + \mathbf{N}_l, \quad (5)$$

where $\mathbf{H}_l$ and $\mathbf{N}_l$ denote the channel state and noise matrices, respectively. The quantity $\mathbf{X}_{\epsilon,l}$ denotes an intersymbol interference (ISI)-corrupted the $N_t \times N_c$ matrix given by

$$\mathbf{X}_{\epsilon,l} = \sum_n \mathbf{X}_{l+n} \mathbf{G}_{\epsilon,n}, \quad (6)$$

where $\mathbf{G}_{\epsilon,n}$ is a $N_c \times N_c$ Toeplitz matrix of pulse shape samples given timing error ϵ, that is

$$\mathbf{G}_{\epsilon,n} = \begin{bmatrix} g_{-nN_c}^\epsilon & g_{-nN_c+1}^\epsilon & g_{-nN_c+2}^\epsilon & \cdots \\ g_{-nN_c-1}^\epsilon & g_{-nN_c}^\epsilon & g_{-nN_c+1}^\epsilon & \ddots \\ g_{-nN_c-2}^\epsilon & g_{-nN_c-1}^\epsilon & g_{-nN_c}^\epsilon & \ddots \\ \vdots & \ddots & \ddots & \ddots \end{bmatrix}. \quad (7)$$

In (7) we used a compact notation of $g_n^\epsilon \triangleq g(nT + \epsilon)$.

Finally, for real-valued modulation, the detection variables for each information symbol $m = 0, \ldots, N_s - 1$ within block l are given by [7]

$$s_m^l = \|\mathbf{H}_l\|^{-2} \Re\{tr(\mathbf{Y}_l^H \mathbf{H}_l \mathbf{A}_m)\}, \quad (8)$$

where $\mathbf{A}_m$ are the code matrices from (1), $\Re\{\cdot\}$ returns the real part of its argument, $tr(\cdot)$ denotes the trace operator, superscript H is the Hermitian transpose operator and $\|\mathbf{H}_l\|$ is the Frobenius norm of $\mathbf{H}_l$. We note that while strictly speaking (8) represents Maximum Likelihood (ML) detection when no timing error is present, we assume the above expression is an approximation to ML detection and verify this assumption via simulations. The projection of s_m^l onto the signal constellation then forms the data decisions denoted by $\hat{a}_m^l$.

III. TIMING ERROR DETECTOR DESIGN

In deriving TED's for real-valued OSTBC, we consider a general expression in the form a linear combination of products $a_n^l s_m^l$, that is

$$\hat{\epsilon}_l = \Re\left(\sum_k \alpha_k a_{n_k}^l s_{m_k}^l\right), \quad (9)$$

where $\{n_k, m_k\}$ are the indices of the data symbols and decision variables within a block l to be chosen accordingly. Note that in (9) we ignore the imaginary component of the estimator.

A. TED S-curve

In [4] the authors derive the expectation $E\{\hat{\epsilon}_l\}$, referred to as the *S-curve*, taken over data and noise for complex valued OSTBC. We summarize the findings of [4] specifically for real modulation formats such as BPSK or PAM.

Referring to the results in [4] and simplifying to real-valued data, one can show that the S-curve for the general TED in (9) is given by

$$E\{\hat{\epsilon}\} = \rho_2 \|\mathbf{H}\|^{-2} tr\{\boldsymbol{\Gamma}\Re(\mathbf{H}^H \mathbf{H})\}, \quad (10)$$

where we have defined a constellation-dependent constant ρ_i for real data given by

$$\rho_i \triangleq E\{a_n^i\}, \quad (11)$$

and a matrix $\boldsymbol{\Gamma}$ given by

$$\boldsymbol{\Gamma} = \sum_k \alpha_k \mathbf{A}_{m_k} \mathbf{G}_\epsilon^T \mathbf{A}_{n_k}^T, \quad (12)$$

where for simplicity $\mathbf{G}_\epsilon$ refers to $\mathbf{G}_{\epsilon,n}$ for $n = 0$. If coefficients $\{\alpha_k, m_k, n_k\}$ are chosen such that $\boldsymbol{\Gamma}$ is in the form of

$$\boldsymbol{\Gamma} = f(\mathbf{G}_\epsilon)\mathbf{I} + \mathbf{D}, \quad (13)$$

where

1) $f(\mathbf{G}_\epsilon)$ is a scalar function of $\mathbf{G}_\epsilon$ that returns a measurement of the timing error
2) $\mathbf{D}$ is an antisymmetric matrix,

then using (10) one can show that [4]

$$E\{\hat{\epsilon}\} = \rho_2 \|\mathbf{H}\|^{-2} tr\{(f(\mathbf{G}_\epsilon)\mathbf{I} + \mathbf{D})\Re(\mathbf{H}^H \mathbf{H})\} = \rho_2 f(\mathbf{G}_\epsilon). \quad (14)$$

We refer to the quantity $f(\mathbf{G}_\epsilon)$ as the *timing error measurement* (TEM). Therefore, if coefficients $\{\alpha_k, m_k, n_k\}$ are selected such that $\boldsymbol{\Gamma}$ satisfies conditions 1) and 2), the TED

$$\boldsymbol{\Phi}_{ijmn} = \begin{cases} (\mathbf{A}_m \mathbf{G}_{\epsilon,0}^T \otimes \mathbf{A}_n \mathbf{G}_{\epsilon,0}^T)(\mathbf{A}_i^T \otimes \mathbf{A}_j^T + \mathbf{A}_j^T \otimes \mathbf{A}_i^T)(\Re(\mathbf{H}^H \mathbf{H}) \otimes \Re(\mathbf{H}^H \mathbf{H})) & i \neq j \\ \left[\sum_l \sum_{k=0}^{N_s-1} (\mathbf{A}_m \mathbf{G}_{\epsilon,l}^T \mathbf{A}_k^T \otimes \mathbf{A}_n \mathbf{G}_{\epsilon,l}^T \mathbf{A}_k^T) + (\frac{\rho_4}{\rho_2^2} - 1)(\mathbf{A}_m \mathbf{G}_{\epsilon,0}^T \mathbf{A}_i^T \otimes \mathbf{A}_n \mathbf{G}_{\epsilon,0}^T \mathbf{A}_i^T) \right] (\Re(\mathbf{H}^H \mathbf{H}) \otimes \Re(\mathbf{H}^H \mathbf{H})) & i = j \end{cases}$$
$$(19)$$

$$\boldsymbol{\Delta}_{ijmn} = \begin{cases} \mathbf{A}_m \boldsymbol{\Psi}_N \Re(\mathbf{H}) \otimes \mathbf{A}_n \boldsymbol{\Psi}_N \Re(\mathbf{H}) + \mathbf{A}_m \boldsymbol{\Psi}_N \Im(\mathbf{H}) \otimes \mathbf{A}_n \boldsymbol{\Psi}_N \Im(\mathbf{H}) & i = j \\ 0 & i \neq j \end{cases}$$
$$(20)$$

---

returns a valid timing error measurement independent of the channel state. We refer to such a TED as being *robust* to channel fading. [1]

In the case where only condition 1) is satisfied, that is $\mathbf{D}$ is an arbitrary matrix with zeros on the main diagonal, then

$$E\{\hat{\epsilon}\} = \rho_2 f(\mathbf{G}_\epsilon) + \delta_{\hat{\epsilon}}, \qquad (15)$$

where $\delta_{\hat{\epsilon}}$ is a TEM *bias* dependent on $\mathbf{H}$. It can be shown using (14) that

$$\delta_{\hat{\epsilon}} = \rho_2 \|\mathbf{H}\|^{-2} \sum_{m=1}^{N_t} \sum_{\substack{i=1 \\ i \neq m}}^{N_t} \sum_{j=1}^{N_r} d_{mi} \Re\left(h_{ij}^* h_{mj}\right), \qquad (16)$$

where we have used d_{mi} to denote the (m,i)th entry of $\mathbf{D}$. The denominator of the bias contains magnitude terms of the channel states, while the numerator is made up of cross products of the channel variables. Thus the average of the bias taken over $\mathbf{H}$ will be relatively small.

In designing a TED for a specific OSTBC, we aim to select coefficients α_k, m_k, n_k to produce a valid timing error measurement $f(\mathbf{G}_\epsilon) = g_{-1}^\epsilon - g_1^\epsilon$, as it represents an accurate difference of threshold crossings estimate of ϵ. In doing so we note that the integer matrices $\mathbf{A}_{m_k}$ and $\mathbf{A}_{n_k}$ in (12) act to shuffle the rows and columns of $\mathbf{G}_\epsilon^T$. Thus the aim is to force the elements g_{-1}^ϵ and g_1^ϵ, located adjacent to the main diagonal of $\mathbf{G}_\epsilon$, to the main diagonal of $\boldsymbol{\Gamma}$ for $k=1$ and $k=2$ respectively. Since the composition of the matrices $\mathbf{A}_{m_k}$ varies for different OSTBC's, the procedure has to be done separately for each code.

B. TED Variance and output SNR

The variance of the TED output, defined by

$$\sigma_{\hat{\epsilon}}^2 = E\{\hat{\epsilon}^2\} - E\{\hat{\epsilon}\}^2, \qquad (17)$$

was solved for the complex OSTBC in [4]. Once again we summarize the results limiting the treatment to real-valued modulation.

Noting (9), the variance of the TED output can be solved by considering individual terms of $E\{\hat{\epsilon}^2\}$, that is $E\{a_i a_j s_m s_n\}$. For real-valued signals the solution is given by [4]

$$E\{a_i a_j s_m s_n\} = \|\mathbf{H}\|^{-4} tr\left\{\rho_2^2 \boldsymbol{\Phi}_{ijmn} + \rho_2 \frac{N_0}{2} \boldsymbol{\Delta}_{ijmn}\right\} \quad (18)$$

[1] In other words, the $tr\{\cdot\}$ operator in (14) returns a full-diversity estimate of ϵ, which removes any dependence on $\mathbf{H}$.

where ρ_i is defined by (11) and matrices $\boldsymbol{\Phi}_{ijmn}$ and $\boldsymbol{\Delta}_{ijmn}$ are given by (19) and (20) where the symbol $\otimes$ represents the Kronecker matrix product.

We note that the first summation in (19) is taken over the ISI-contributing blocks, and will converge since $\mathbf{G}_{\epsilon,l} \to \mathbf{0}$ as $|l| \to \infty$. The components of the matrix $\boldsymbol{\Psi}_N$, of dimensions $N_c N_c \times N_r N_r$ in (20), are given by

$$\boldsymbol{\Psi}_N(i,j) = \begin{cases} 1 & i = nN_r + n + 1, j = mN_c + m + 1 \\ 0 & elsewhere \end{cases}$$
$$(21)$$

for $n = 0, \ldots, N_r - 1$ and $m = 0, \ldots, N_c - 1$. The final expression for $E\{\hat{\epsilon}^2\}$ will be of the form

$$E\{\hat{\epsilon}^2\} = \|\mathbf{H}\|^{-4} tr\left\{\rho_2^2 \boldsymbol{\Sigma}_{\boldsymbol{\Phi}} + \rho_2 \frac{N_0}{2} \boldsymbol{\Sigma}_{\boldsymbol{\Delta}}\right\}, \qquad (22)$$

with the matrices $\boldsymbol{\Sigma}_{\boldsymbol{\Phi}}$ and $\boldsymbol{\Sigma}_{\boldsymbol{\Delta}}$ corresponding to the linear combination of $\boldsymbol{\Phi}_{ijmn}$ and $\boldsymbol{\Delta}_{ijmn}$ respectively, as determined by the polynomial expansion in $E\{\hat{\epsilon}^2\}$ for a particular TED. Expressions for specific TED will be shown in Section III-C where examples of TED are presented.

Using the solutions for the S-curve in (10) and TED variance in (17) and (22), we can define the TED SNR defined as

$$SNR_{TED} = \frac{E^2\{\hat{\epsilon}\}}{\sigma_{\hat{\epsilon}}^2}. \qquad (23)$$

C. Timing Error Detectors for Real Valued OSTBC

This section presents examples of TED's for real-valued 2-, 3- and 4-transmit antenna OSTBC. As proposed in [5], a TED for 2-transmit antenna OSTBC (Alamouti encoding) has the form of

$$\hat{\epsilon}_{(2)} = \Re\{a_0 s_1 - a_1 s_0\}. \qquad (24)$$

The same expression can be used for the case of real data. Substituting the coefficients into (12), we obtain

$$\boldsymbol{\Gamma}_{(2)} = \begin{bmatrix} g_{-1}^\epsilon - g_1^\epsilon & -2g_0^\epsilon \\ 2g_0^\epsilon & g_{-1}^\epsilon - g_1^\epsilon \end{bmatrix}, \qquad (25)$$

that is, $f(\mathbf{G}_\epsilon) = g_{-1}^\epsilon - g_1^\epsilon$. We note that matrix $\boldsymbol{D}$, as defined by (13), satisfies the antisymmetry condition. Thus, the TED in (24) will yield a TEM with $E\{\hat{\epsilon}_{(2)}\} = \rho_2(g_{-1}^\epsilon - g_1^\epsilon)$ and bias $\delta_{\hat{\epsilon}_{(2)}} = 0$.

The variance of the TED in (24) can be obtained from (17) and (22) with $\boldsymbol{\Sigma}_{\boldsymbol{\Phi}}$ and $\boldsymbol{\Sigma}_{\boldsymbol{\Delta}}$ given by

$$\boldsymbol{\Sigma}_{\boldsymbol{\Phi}} = \boldsymbol{\Phi}_{0011} + \boldsymbol{\Phi}_{1100} - 2\boldsymbol{\Phi}_{0101} \qquad (26)$$

and

$$\boldsymbol{\Sigma}_{\boldsymbol{\Delta}} = \boldsymbol{\Delta}_{0011} + \boldsymbol{\Delta}_{1100}. \qquad (27)$$

A rate-one code for 4-transmit antenna OSTBC is given by [9]

$$\mathbf{X}_{(4)} = \begin{bmatrix} a_0 & -a_1 & -a_2 & -a_3 \\ a_1 & a_0 & a_3 & -a_2 \\ a_2 & -a_3 & a_0 & a_1 \\ a_3 & a_2 & -a_1 & a_0 \end{bmatrix}. \tag{28}$$

Referring to (12), we note that selecting $n_1 = 2$ and $m_1 = 1$ will cause matrices $\mathbf{A}_1$ and $\mathbf{A}_2^T$ to force the main diagonal of $\mathbf{\Gamma}$ to be $\{g_{-1}^\epsilon, -g_{-3}^\epsilon, g_3^\epsilon, -g_1^\epsilon\}$. Similarly, selecting $n_2 = 1$ and $m_2 = 2$ will contribute $\{g_1^\epsilon, -g_{-3}^\epsilon, g_{-3}^\epsilon, -g_{-1}^\epsilon\}$. By subtracting the $k = 2$ term from the $k = 1$ term, we obtain the main diagonal of $\mathbf{\Gamma}$ of $\{g_{-1}^\epsilon - g_1^\epsilon, g_3^\epsilon - g_{-3}^\epsilon, g_3^\epsilon - g_{-3}^\epsilon, g_{-1}^\epsilon - g_1^\epsilon\}$. In order to force the TEM of $g_{-1}^\epsilon - g_1^\epsilon$ onto the 2nd and 3rd positions of the diagonal, we include two additional terms in (12). For $k = 3$ and $k = 4$ we select $n_3 = 3$, $m_3 = 0$ and $n_4 = 0$, $m_4 = 3$, respectively. Subtracting these will result in the contribution to the diagonal of $\mathbf{\Gamma}$ of $\{g_3^\epsilon - g_{-3}^\epsilon, g_{-1}^\epsilon - g_1^\epsilon, g_{-1}^\epsilon - g_1^\epsilon, g_3^\epsilon - g_{-3}^\epsilon\}$. Therefore combining terms $k = 1, \ldots, 4$, equivalent to a TED in the form of

$$\hat{\epsilon}_{(4)} = \Re\{a_2 s_1 - a_1 s_2 + a_3 s_0 - a_0 s_3\}, \tag{29}$$

will result in $\mathbf{\Gamma}$ given by

$$\mathbf{\Gamma}_{(4)} = \begin{bmatrix} \gamma_{ii} & \gamma_{12} & 0 & 0 \\ -\gamma_{12} & \gamma_{ii} & 0 & 0 \\ 0 & 0 & \gamma_{ii} & \gamma_{12} \\ 0 & 0 & -\gamma_{12} & \gamma_{ii} \end{bmatrix}, \tag{30}$$

where we have defined

$$\gamma_{ii} = g_{-1}^\epsilon - g_1^\epsilon - g_{-3}^\epsilon + g_3^\epsilon \tag{31}$$

and

$$\gamma_{12} = 2g_{-2}^\epsilon + 2g_2^\epsilon. \tag{32}$$

Examining (30) we see that $\mathbf{D}$ satisfies condition 2) and thus the TED $\hat{\epsilon}_{(4)}$ is robust. The S-curve is given by

$$E\{\hat{\epsilon}_{(4)}\} = \rho_2(g_{-1}^\epsilon - g_1^\epsilon - g_{-3}^\epsilon + g_3^\epsilon), \tag{33}$$

with timing measurement bias $\delta_{\hat{\epsilon}} = 0$. We note that compared to the $N_t = 2$ code, the TED S-curve contains an additional term of $-g_{-3}^\epsilon + g_3^\epsilon$. While this term will reduce the value of the error estimate, for small values of ϵ its effect will be negligible.

The variance of the TED in (29) can be obtained from (17) and (22) with $\mathbf{\Sigma}_\Phi$ and $\mathbf{\Sigma}_\Delta$ given by

$$\mathbf{\Sigma}_\Phi = \mathbf{\Phi}_{1122} + \mathbf{\Phi}_{2211} + \mathbf{\Phi}_{3300} + \mathbf{\Phi}_{0033}$$
$$- 2(\mathbf{\Phi}_{2112} - \mathbf{\Phi}_{2310} + \mathbf{\Phi}_{2024} + \mathbf{\Phi}_{1320} - \mathbf{\Phi}_{1034} + \mathbf{\Phi}_{3003}) \tag{34}$$

and

$$\mathbf{\Sigma}_\Delta = \mathbf{\Delta}_{1122} + \mathbf{\Delta}_{2211} + \mathbf{\Delta}_{3300} + \mathbf{\Delta}_{0033} \tag{35}$$

An equivalent code for $N_t = 3$ can be obtained by deleting the last row in (28). The TED in (29) results in the same S-curve and variance when applied to the $N_t = 3$ code.

As a final note we point out that $\mathbf{\Sigma}_\Phi$ and $\mathbf{\Sigma}_\Delta$, given by (19) and (20), depend on the channel state. In computing the variance of the estimator, the expectation over $\mathbf{H}$ must be evaluated numerically, as will be done in Section IV-A.

IV. SIMULATION RESULTS

We present simulation results evaluating the performance of the TED in (29) for 4-transmit antenna OSTBC in (28). Analytical expression for TED SNR is evaluated and confirmed via simulation. BER results are also shown, followed by the analysis of the range of timing drift tracked by the timing loop.

A. TED Properties

Figure 2 shows the TED SNR as defined by (23) for $\hat{\epsilon}_{(4)}$ with $N_r = 2$ receive antennas, with $E_s/N_0 = 0$ dB, 10 dB, 20 dB and 30 dB. The variance term in (23) was obtained by evaluating (17) with (22), (34) and (35), and averaged over 10^4 channel instances. In addition to the theoretical curves, simulated values were obtained with data sampled at a fixed timing error ϵ and timing correction disabled. The error variance was calculated by averaging $(\epsilon - \hat{\epsilon})^2$ over all code blocks transmitted.
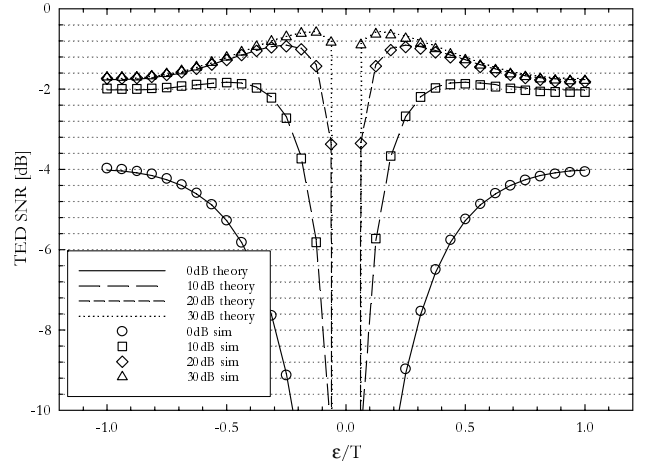

Fig. 2. TED output SNR

For $\epsilon = 0$, where no correction is needed, the $E\{\hat{\epsilon}\} = 0$ and thus the TED SNR is zero. We note that for moderate E_s/N_0, the TED SNR peaks at a normalized timing error of below $\epsilon/T = 0.25$, which is the usual operating region of the timing loop. This result is consistent with the findings for $N_t = 2$ complex OSTBC reported in [6]. In the case of a large timing offset, the estimation variance is large, and thus the TED SNR decreases.

B. BER Performance

For the simulations evaluating overall system performance, the data streams on each branch were passed through an RRC filter with a rolloff of $\beta_{MF} = 0.35$. The normalized Doppler frequency was set to $f_D T = 0.01$. We assume that the receiver has performed coarse timing acquisition, which would typically have been done using a training sequence. The timing drift was simulated by perturbing the sampling phase τ_l. The interval between timing slips, measured in symbol intervals and denoted by N_τ, was modeled by a Gaussian random variable, with a mean of $\bar{N}_\tau$ and with a variance of $\sigma_{N_\tau}^2 = 0.1\bar{N}_\tau$. The drift direction was random and equiprobable, with

the step size fixed to $T/8$. The resulting mean timing error bandwidth, normalized to the symbol duration T, is given by

$$\bar{B}_\tau T = \frac{T/8}{\bar{N}_\tau T} = \frac{1}{8\bar{N}_\tau}.$$

BER results were obtained for $\bar{B}_\tau T = 1 \times 10^{-4}$. Since the focus of the investigation is the tracking performance of the detector, the timing estimation was done without the knowledge of the data symbols at the receiver. Hence the data symbols a_m in (29) were replaced by their estimates $\hat{a}_m$. The timing measurement was passed through a first-order IIR filter, whose output denoted by $\hat{\epsilon}'_l$, is given by

$$\hat{\epsilon}'_l = \alpha \hat{\epsilon}'_{l-1} + (1-\alpha)\hat{\epsilon}_l, \tag{36}$$

with the loop constant set to $\alpha = 0.95$. When $\hat{\epsilon}'_l$ exceeded a threshold value, set to $\epsilon_{th} = 0.25$, the timing correction $\hat{\tau}_l$ was adjusted by $T/8$, depending on the polarity of the error estimate.

Figure 3 shows BPSK BER plots, including reference curves for ideal timing. The results demonstrate that the receiver
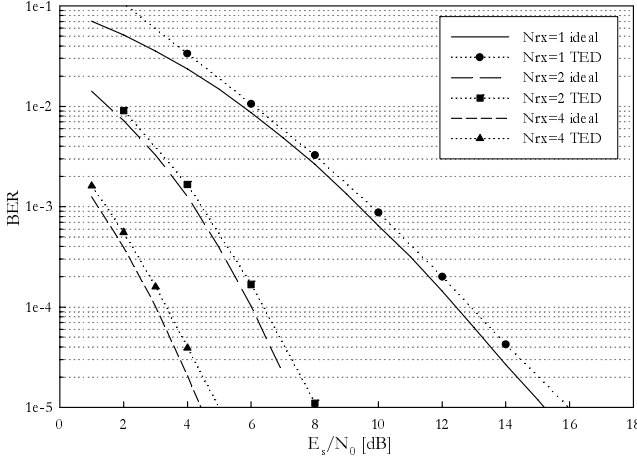

Fig. 3.   BER, TED for $N_t = 4$ BPSK

tracks the timing variation with a performance drop of under 0.5 dB. This result justifies the use of (8) as an approximation to the ML-detection rule. We note that for low SNR, particularly for $N_r = 1$, the stability can be improved by increasing the loop filter coefficient α and the threshold ϵ_{th}.

C. Performance as a Function of Timing Bandwidth

Figure 4 shows the BER as a function of timing bandwidth $\bar{B}_\tau T$ for $N_r = 2$ receiver operating at SNR of 8, 10 and 12 dB. All parameters were set as described in Section IV-B.

We note that the receiver is able to track timing up to approximately $\bar{B}_\tau T = 1 \times 10^{-3}$ with little loss due to timing recovery.

V. CONCLUSION

The paper summarized timing error detector design for real-valued OSTBC, giving theoretical expressions for the S-curve, variance and TED SNR. We have presented examples
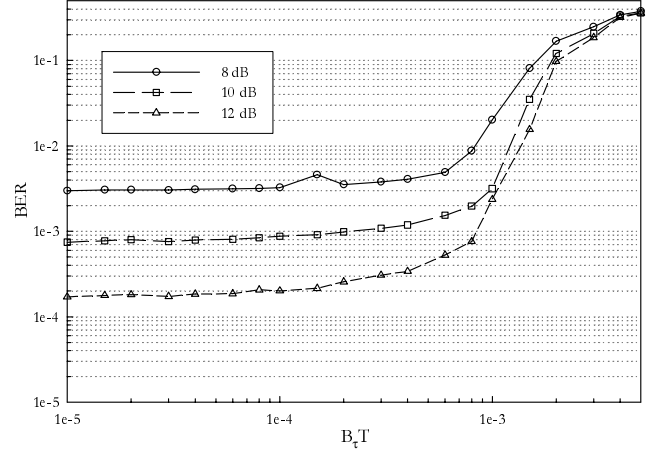

Fig. 4.   BER vs normalized timing bandwidth $\bar{B}_\tau T$ ($N_t = 4$, $N_r = 2$)

of TED's for 2-, 3- and 4-transmit antenna BPSK codes. Simulations were used to confirm the theoretical results, as well as to evaluate the overall system performance. Bit-error-rate curves were presented, showing loss due to timing recovery of under 0.5 dB. Finally, it was shown that the receiver is able to track timing drift of up to $\bar{B}_\tau T = 10^{-3}$.

REFERENCES

[1] A.F.Naguib, V.Tarokh, N.Seshadri, and R.Calderbank. A space-time coding modem for high-data-rate wireless communications. *IEEE J. Select. Areas Commun.*, 16(8):1459–1478, October 1998.

[2] Y.-C.Wu and S.C.Chan. On the symbol timing recovery in space-time coding systems. In *Proc. IEEE WCNC*, March 2003.

[3] Y.-C.Wu, S.C.Chan, and E.Serpedin. Symbol-timing synchronization in space-time coding systems using orthogonal training sequences. In *Proc. IEEE WCNC*, March 2004.

[4] P.A.Dmochowski and P.J.McLane. Timing error detector design for orthogonal space-time block codes. *(to be submitted)*.

[5] P.A.Dmochowski and P.J.McLane. Robust timing epoch tracking for Alamouti space-time coding in flat Rayleigh fading MIMO channels. In *Proc. IEEE ICC*, pages 2397 – 2401, 16-20 May 2005.

[6] P.A.Dmochowski and P.J.McLane. On the properties of robust timing error detector for Alamouti space-time coding in flat Rayleigh fading MIMO channels with randomly distributed timing drift. In *Proc. IEEE GLOBECOM*, pages 193 – 198, 28 Nov.-2 Dec. 2005.

[7] G.Ganesan and P.Stoica. Space-time block codes: A maximum SNR approach. *IEEE Trans Inf. Theory*, 47(4):1650–1656, May 2001.

[8] G.L.Stuber. *Principles of Mobile Communications.* Kluwer Academic Publishers, 2001.

[9] V.Tarokh, H. Jafarkhani, and A.R.Calderbank. Space-time block codes from orthogonal designs. *IEEE Trans Inf. Theory*, 45(5):1456–1467, July 1999.

[10] S.M.Alamouti. A simple transmit diversity technique for wireless communication. *IEEE J. Select. Areas Commun.*, 16(8):1451–1458, October 1998.